Unsupervised Domain Adaptation for Position-Independent IMU Based Gait Analysis

Fangzhi Mu, Xiao Gu, Yao Guo, and Benny Lo

***Abstract*— Inertial measurement units (IMUs) together with advanced machine learning algorithms have enabled pervasive and intelligent gait analysis systems. However, the body positions of IMUs are easy to change or difficult to control across different trials, causing signal variations. Such heterogeneity contributes to biased underlying distribution of training and testing data, and largely constrains the generalization ability of a computational gait analysis model. In this paper, we developed a position-independent IMU based gait analysis framework based on unsupervised domain adaptation. It functions by transferring knowledge from the trained data positions to a novel position without labels. We tested our framework on gait event detection and pathological gait pattern recognition tasks based on different computational models and achieved consistently high performance on both tasks.**

I. Introduction

Recent advances in wearable sensing have provided low-cost and pervasive solutions for gait monitoring [1]. They aim to explore relevant biomechanical features in free-living environments and subsequently discover the relationship between gait disorders and their associated musculoskeletal or neurological diseases. One of the representative sensors is the inertial measurement unit (IMU). It is a kind of inexpensive and portable sensor which allows continuous ambulatory acquisition of three-dimensional motion signals [2]. IMUs have been widely used in gait analysis for a widely range of clinical applications [3], [4], [5].

There have been increasing interests in integrating advanced machine learning or deep learning algorithms with IMUs for automatic intelligent gait analysis systems. They function by utilizing a computational model trained from a collection of training data for a certain task. However, most existing algorithms are limited when distribution discrepancies exist between training and testing data. In fact, such a problem are common in IMUs, as their signals are sensitive to the positions while IMU positions are are easy to change and difficult to precisely control in real world settings [6]. The placement or orientation of a IMU may be different across each trial for a subject, and the related mis-orientation, transitional shift or even displacement affects recorded data patterns [6].

Research efforts have been devoted to addressing this issue either based on anatomical calibration [7], [8], [9] or engineering position-independent features [10], [11]. The former requires pre-trial functional calibration through pre-defined postures which however is not suitable for 24/7 continuous monitoring. Attempts of the latter one including magnitude and weighted sum of accelerator signals [10] and transforming raw accelerator data into canonical world coordinates based on the magnetometer data[11]. However, the raw data are prone to noises and biases, and sensor characteristics cannot be well aligned through simple projection.

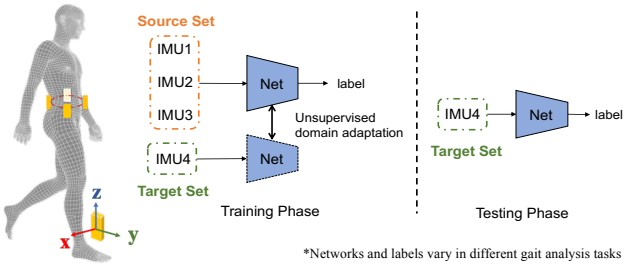

Fig. 1. Framework of single positon-independent IMU based gait analysis.

In transfer learning field, the discrepancy of data distributions, normally referred to as domains, is called domain shift problem. Unsupervised domain adaptation (UDA) is an emerging transductive transfer learning technique for mitigating such shifts, adapting learned computational model from source to unlabelled target domains [12]. It reduces the efforts of labelling on the target domains while maintaining good performance across domains. It has been investigated a lot in computer vision field while receiving less attention in human signals, especially in human gaits.

In this paper, we proposed a novel end-to-end position-independent IMU based gait analysis framework with the help of unsupervised domain adaptation. We built our model based on two advanced methods, domain adversarial neural networks (DANN [13]) and the extended multi-source DANN (MS-DANN). As shown in Fig. 1, our framework can automatically align the IMU data from source positions and unlabelled data from the target position via our unsupervised domain adaptation training. Our proposed method can work well on the novel target position without fine-tuning for both gait event detection and abnormal gait pattern recognition tasks.

II. Methodologies

A. Unsupervised Domain Adaptation

Unsupervised domain adaptation tries to transfer knowledge learned from source domains to unlabelled target domains. Given a computational model $M : X \mapsto Y$, X refers to raw data and Y its corresponding label space. For unsupervised domain adaptation problem, we denote the source domain data of n_S samples as $\mathcal{D}_S = \{(x_i^s, y_i^s)\}_i^{n_S}$

[1]Fangzhi Mu, Xiao Gu, Yao Guo and Benny Lo are with the Hamlyn Centre, Institute of Global Health Innovation, Imperial College London, London SW7 2AZ, United Kingdom. {f.mu19, xiao.gu17, yao.guo, benny.lo}@imperial.ac.uk

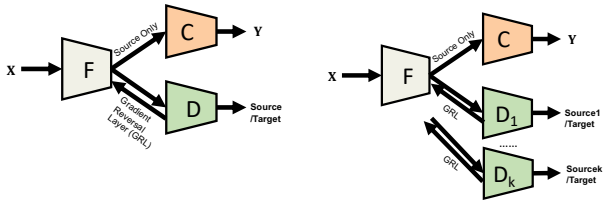

(a) DANN (b) MS-DANN

Fig. 2. Illustrations of architectures of DANN and MS-DANN.

and the target domain data of n_T unlabelled samples as $D_T = \{x_j^T\}_j^{n_T}$. The joint distributions between source $\mathcal{P}_S(X,Y)$ and target $\mathcal{P}_T(X,Y)$ are different. Unsupervised domain adaptation aims to utilize D_S and D_T to train a model that generalizes on target as well.

1) Domain Adversarial Neural Network: Domain adversarial neural network (DANN [13]) aims to project data from two different domains into a common subspace via adversarial training. As shown in Fig. 2, the basic DANN architecture consists of three components, the feature extractor F, the domain classifier D and the task specific classifier C. C is responsible for extracting discriminative features for specific tasks. The domain classifier D is expected to classify different domains while F is expected to extract features that are discriminative for C but cannot be distinguished by D. This adversarial setting is realized by a gradient reversal layer between F and D, which negates the gradient during propagation.

The loss function of this network is as follows,

$$\begin{aligned}\mathbb{E}_{DANN} &= \lambda_C \sum_{D_S} \mathcal{L}_C - \lambda_D \sum_{D_S, D_T} \mathcal{L}_D \\ &= \lambda_C \sum_{D_S} \mathcal{L}_C(C(F(x_i)), y_i) \\ &- \lambda_D \sum_{D_S, D_T} CE(D(F(x_i), d_i))\end{aligned} \tag{1}$$

where CE is the cross-entropy loss, and d_i refers to the corresponding domain label. To be specific, $\mathcal{L}_C$ may differ across different gait analysis tasks.

The optimization objective of DANN is as follows,

$$\hat{\theta}_F, \hat{\theta}_C, \hat{\theta}_D = \arg \min_{\theta_F, \theta_C} \max_{\theta_D} \mathbb{E}_{DANN} \tag{2}$$

2) Multi-Source Domain Adversarial Training: When multiple source domains $\{D_{S_k}\}$ exist, treating multiple sources as a single one may lead to suboptimal solutions, as different sources own their unique distributions [14]. To address it, Zhao *et al.* [14] and Pei *et al.* [15] extended the structure of DANN to a multi-source version by adding multiple domain classifier branches C_k for each source domain. Their proposed architectures are able to effectively align data distribution across multiple domains and extract domain-invariant features.

In our case, the training data comes from IMUs with multiple positions, which matches well with the scenarios of applying multi-source domain adaptation. Therefore, we adopted an architecture similar to [15], [14], called MS-DANN as shown in Fig. 2. The loss function is as follows,

$$\begin{aligned}\mathbb{E}_{MSDANN} &= \lambda_C \sum_{\{D_{S_k}\}} \mathcal{L}_C - \lambda_D \sum_{D_S, D_T} \mathcal{L}_D \\ &= \lambda_C \sum_{\{D_{S_k}\}} \mathcal{L}_C(C(F(x_i)), y_i) \\ &- \lambda_D \sum_k \sum_{\{D_{S_k}\}, D_T} CE(D_k(F(x_i), d_i))\end{aligned} \tag{3}$$

Its minmax optimization objective is similar to Equation 2.

B. Task Specific Architectures

Customizing the aforementioned architectures, we explored two different gait analysis tasks of interest, real-time gait event detection and pathological gait pattern recognition with different backbone networks.

1) Real-Time Gait Event Detection: Accurate gait event detection is fundamental for extracting some important spatial-temporal gait parameters, like stride width, walking speed and walking symmetry [16], [17]. In this paper, four key gait events are considered, which are left and right, heel-strike (LHS and RHS) and toe-off (LTO and RTO) separately. Based on these gait events, a gait cycle can be divided to four phases (double support1, right support, double support2, left support). We perform classification on gait phases firstly to avoid class imbalance problem between gait events and non-gait events, and subsequently convert detected phases into gait events.

We applied Bidirectional Long-Short-Term-Memory (BiLSTM) as F to realize sequence to sequence phase classification following previous work [18]. The input is each time segment $x \in \mathbb{R}^{l \times c}$ and the output is $y \in \mathbb{R}^l$, where l is the segment length, and c is the input signal channel number.

2) Pathological Gait Pattern Recognition: The generalization performance of our model for pathological gait classification are also investigated. Following our previous work [1], [19], six different walking patterns are involved, which are normal, pronation, supination, asymmetric, toe-in and toe-out.

We used One-Dimensional Convolutional Neural Network (1D-CNN) similar to [20] as F to perform sequence classification task. The input signal is each gait cycle signal segmented by annotated right heel strikes, $x \in \mathbb{R}^{l \times c}$, where l is the normalized length and c is the channel number. The output is the gait pattern class $y \in \mathbb{R}$.

III. Experiment Settings

A. Data Collection

We collected data[1] with subjects (7 subjects, 1 female) walking on a treadmill and four IMUs (Delsys Inc., Boston, MA) attached to the body surface around the waist (1-front, 2-back, 3-left, 4 right), as shown in Fig. 1. The recruited subjects were instructed to perform six walking conditions by imitation or insole assistance [19]. The human skeleton data was recorded simultaneously via Vicon (Vicon Inc, Los Angeles, CA) to provide ground truth gait event labels. These

[1]This experiment was approved by XXX

two modalities were synchronized via Vicon LockLab, and the sampling frequency of the whole system is $100Hz$. For each walking condition, each subject ran 5 trials with a duration of around 30s each.

B. Network Details

Our adversarial neural network components C and D are both made up of three concatenated fully connected layers. $\mathcal{L}_C$ in Equation 1&3 adopts cross-entropy loss. F follows the specific structure for each task (LSTM: layers-3, hidden size-128; 1D-CNN: 4 layers,channel-18→36→72→144,kernel-3,stride-2). λ_C=1, λ_D=1, l=128, c=9 for both tasks. For each training session, we randomly extracted 70% from source and target data for training, and 30% from source for validation, 30% from target for testing.

IV. Results

A. Real-Time Gait Event Detection

We applied cross-position validation protocol. In each session, we randomly selected three positions as source data, and the held-out one as target. For gait event detection, Fig. 3 shows the results of gait phase classification. We compared the results of BilSTM (simply training on source data), BiLSTM+DANN, and BiLSTM+MS-DANN. Subsequently, we converted the estimated phase to gait event, and the frame shift error of detected gait events are reported in Table I. Due to large error of inferring gait phases with the results of BiLSTM, its estimated gait phases cannot be successfully converted to gait events directly, which are not reported accordingly.

The improved phase classification of DANN and MS-DANN in Fig. 3 shows the effectiveness of our proposed methods, while in turn the inferior performance of pure BiLSTM highlights the data bias. On the other hand, in both Fig. 3 and Table I, the slightly better performance of MS-DANN versus DANN demonstrates MS-DANN's higher capability of handling multiple source domains.

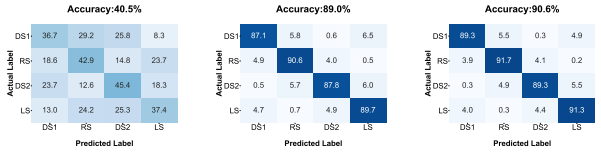

(a) BiLSTM (b) BiLSTM+DANN (c) BiLSTM+MSDANN

Fig. 3. Confusion matrices of gait phase classification via cross-position validation. (DS1: double support1; RS: right support; DS2: double support2; LS: left support)

TABLE I

Mean frame shift error of detected gait events via cross-position validation

S → T	BiLSTM*	BiLSTM+DANN				BiLSTM+MS-DANN			
	-	lhs	lto	rhs	rto	lhs	lto	rhs	rto
1,2,3→4	-	4.68	4.54	6.88	4.80	**3.72**	3.52	3.82	3.77
1,2,4→3	-	3.82	5.61	4.42	4.66	3.99	4.24	3.60	**3.40**
1,3,4→2	-	**2.55**	3.37	2.96	3.93	2.81	4.07	3.08	3.26
2,3,4→1	-	3.01	4.79	4.57	4.73	3.72	**3.00**	3.31	4.06

B. Pathological Gait Pattern Recognition

With the same validation protocol, the confusion matrices of pathological gait pattern recognition are shown in Fig. 4. In Table II, three classification metrics, Recall, Precision, and F1 are reported. They present similar performance as that of gait event detection in Section IV-A.

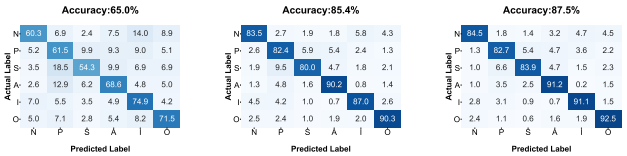

(a) CNN (b) CNN+DANN (c) CNN+MSDANN

Fig. 4. Confusion matrices of gait pattern classification via cross-position validation. (N:Normal; P: Pronation; S:Supination; A: Asymmetric; I: Toe-in; O: Toe-out.)

TABLE II

Classification results (Recall, Precision and F1) of six gait types via cross-position validation

S → T	CNN			CNN+DANN			CNN+MS-DANN		
	Rec	Prec	F1	Rec	Prec	F1	Rec	Prec	F1
1,2,3→4	0.57	0.64	0.60	0.84	0.85	0.85	**0.86**	**0.88**	**0.87**
1,2,4→3	0.64	0.70	0.64	0.84	0.85	0.84	**0.87**	**0.87**	**0.87**
1,3,4→2	0.64	0.67	0.65	0.84	0.83	0.83	**0.86**	**0.87**	**0.86**
2,3,4→1	0.59	0.66	0.61	**0.84**	0.85	**0.85**	0.83	**0.87**	**0.85**

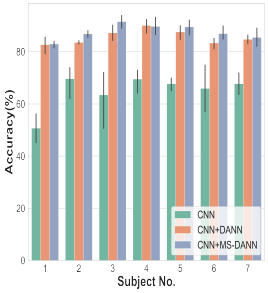

Fig. 5. Gait pattern classification accuracy for each subject via cross-position validation.

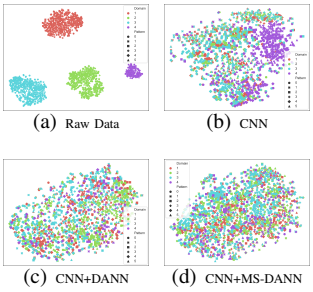

Fig. 6. The t-SNE visualizations of raw data and the embedded features extracted from different methods when using 1,2,3 for training and 4 for testing.

In Fig. 5, the gait pattern classification results of each subject are shown. MS-DANN and DANN achieves consistently high scores across different subjects, and MS-DANN shows better performance than the single-source one.

Fig. 6 shows the t-SNE visualizations of raw data and the embedded features extracted from different methods. It can be observed that the raw data (Fig. 6(a)) have distinct distribution shift across different domains. Without UDA, the target features (purple) remain outside the source ones as shown in Fig. 6(b), whereas a uniform distribution can be observed in Fig. 6(c)&6(d).

V. Discussion and Conclusion

In this paper, we proposed an end-to-end single position-independent IMU based gait analysis framework based on unsupervised domain adaptation. It established knowledge transfer across labelled data from source positions and unlabelled data from a novel target position. We have validated its effectiveness on different gait analysis tasks and different deep learning models and achieved consistently high performance with our methods. Next step is to investigate the heterogeneous difference across different subjects and different walking scenarios, while cascading gait event detection and gait pattern classification to construct a complete gait analysis system.

REFERENCES

[1] X. Gu, F. Deligianni, B. Lo, W. Chen, and G.-Z. Yang, "Markerless gait analysis based on a single rgb camera," in *2018 IEEE 15th International Conference on Wearable and Implantable Body Sensor Networks (BSN)*. IEEE, 2018, pp. 42–45.

[2] R. Caldas, M. Mundt, W. Potthast, F. B. de Lima Neto, and B. Markert, "A systematic review of gait analysis methods based on inertial sensors and adaptive algorithms," *Gait & posture*, vol. 57, pp. 204–210, 2017.

[3] C. Caramia, D. Torricelli, M. Schmid, A. Muñoz-Gonzalez, J. Gonzalez-Vargas, F. Grandas, and J. L. Pons, "Imu-based classification of parkinson's disease from gait: A sensitivity analysis on sensor location and feature selection," *IEEE journal of biomedical and health informatics*, vol. 22, no. 6, pp. 1765–1774, 2018.

[4] F. A. Storm, C. J. Buckley, and C. Mazzà, "Gait event detection in laboratory and real life settings: Accuracy of ankle and waist sensor based methods," *Gait & posture*, vol. 50, pp. 42–46, 2016.

[5] D. Jarchi, C. Wong, R. M. Kwasnicki, B. Heller, G. A. Tew, and G.-Z. Yang, "Gait parameter estimation from a miniaturized ear-worn sensor using singular spectrum analysis and longest common subsequence," *IEEE Transactions on Biomedical Engineering*, vol. 61, no. 4, pp. 1261–1273, 2014.

[6] R. Saeedi and A. Gebremedhin, "A signal-level transfer learning framework for autonomous reconfiguration of wearable systems," *IEEE Transactions on Mobile Computing*, 2018.

[7] E. Palermo, S. Rossi, F. Marini, F. Patanè, and P. Cappa, "Experimental evaluation of accuracy and repeatability of a novel body-to-sensor calibration procedure for inertial sensor-based gait analysis," *Measurement*, vol. 52, pp. 145–155, 2014.

[8] L. S. Vargas-Valencia, A. Elias, E. Rocon, T. Bastos-Filho, and A. Frizera, "An imu-to-body alignment method applied to human gait analysis," *Sensors*, vol. 16, no. 12, p. 2090, 2016.

[9] X. Robert-Lachaine, H. Mecheri, C. Larue, and A. Plamondon, "Accuracy and repeatability of single-pose calibration of inertial measurement units for whole-body motion analysis," *Gait & posture*, vol. 54, pp. 80–86, 2017.

[10] A. Tarashansky, H. Vathsangam, and G. S. Sukhatme, "A study of position independent algorithms for phone-based gait frequency detection," in *2014 36th Annual International Conference of the IEEE Engineering in Medicine and Biology Society*. IEEE, 2014, pp. 5984–5987.

[11] Q. Cheng, J. Juen, Y. Li, V. Prieto-Centurion, J. A. Krishnan, and B. R. Schatz, "Gaittrack: Health monitoring of body motion from spatio-temporal parameters of simple smart phones," in *Proceedings of the International Conference on Bioinformatics, Computational Biology and Biomedical Informatics*, 2013, pp. 897–906.

[12] W. M. Kouw and M. Loog, "A review of domain adaptation without target labels," *IEEE transactions on pattern analysis and machine intelligence*, 2019.

[13] Y. Ganin, E. Ustinova, H. Ajakan, P. Germain, H. Larochelle, F. Laviolette, M. Marchand, and V. Lempitsky, "Domain-adversarial training of neural networks," *The Journal of Machine Learning Research*, vol. 17, no. 1, pp. 2096–2030, 2016.

[14] H. Zhao, S. Zhang, G. Wu, J. M. Moura, J. P. Costeira, and G. J. Gordon, "Adversarial multiple source domain adaptation," in *Advances in neural information processing systems*, 2018, pp. 8559–8570.

[15] Z. Pei, Z. Cao, M. Long, and J. Wang, "Multi-adversarial domain adaptation," in *Thirty-Second AAAI Conference on Artificial Intelligence*, 2018.

[16] J.-Y. Jung, W. Heo, H. Yang, and H. Park, "A neural network-based gait phase classification method using sensors equipped on lower limb exoskeleton robots," *Sensors*, vol. 15, no. 11, pp. 27 738–27 759, 2015.

[17] S. R. Hundza, W. R. Hook, C. R. Harris, S. V. Mahajan, P. A. Leslie, C. A. Spani, L. G. Spalteholz, B. J. Birch, D. T. Commandeur, and N. J. Livingston, "Accurate and reliable gait cycle detection in parkinson's disease," *IEEE Transactions on Neural Systems and Rehabilitation Engineering*, vol. 22, no. 1, pp. 127–137, 2013.

[18] Ł. Kidziński, S. Delp, and M. Schwartz, "Automatic real-time gait event detection in children using deep neural networks," *PloS one*, vol. 14, no. 1, p. e0211466, 2019.

[19] Y. Guo, F. Deligianni, X. Gu, and G.-Z. Yang, "3-d canonical pose estimation and abnormal gait recognition with a single rgb-d camera," *IEEE Robotics and Automation Letters*, vol. 4, no. 4, pp. 3617–3624, 2019.

[20] S.-M. Lee, S. M. Yoon, and H. Cho, "Human activity recognition from accelerometer data using convolutional neural network," in *2017 ieee international conference on big data and smart computing (bigcomp)*. IEEE, 2017, pp. 131–134.